Electronic Gas-Phase Spectra of Larger Polyacetylene Cations

Anatoly Dzhonson, Evan B. Jochnowitz, and John P. Maier*

Department of Chemistry, University of Basel, Klingelbergstrasse 80, CH-4056 Basel, Switzerland

Received: November 10, 2006; In Final Form: December 19, 2006

The origin bands of the A $^2\Pi-X\ ^2\Pi$ electronic transition for three new linear polyacetylene cation chains, $HC_{12}H^+$, $HC_{14}H^+$, and $HC_{16}H^+$, have been recorded in the gas phase at ~30 K, located at 924.7, 1034.6, and 1144.0 nm. The absorption spectra were observed using a two-color two-photon ion-photodissociation experiment that utilizes the cooling capabilities of a 22-pole ion trap. Such spectra allow a direct comparison between laboratory and astrophysical data; however, no matches were found between the experimentally determined origin bands and the known diffuse interstellar bands.

Introduction

A number of polyacetylene cation chains have been studied in neon matrices[1,2] and in the gas phase.[3−8] Interest in these species stems from the observation of hydrocarbons in combustion and interstellar environments.[9−12] In terms of astrophysical relevance, large carbon chains are often speculated as being possible carriers of the unidentified absorptions in diffuse interstellar clouds. In this vein, spectroscopic studies in the laboratory are essential for astronomical assignments and help in the detection of new species in the interstellar medium. Approximately 100 of the more than 130 molecules that have been detected in the interstellar medium or circumstellar shells contain carbon. Because microwave spectra of the linear polyacetylene cations are not available due to their centrosymmetric nature, electronic spectroscopy offers a means of identification in the diffuse clouds.

It is crucial for a molecule to have a strong electronic transition moment to assist astrophysical detection. One way to search for strong optical transitions is to examine longer hydrocarbon chains for which the oscillator strength scales with size.[13] Carbon atoms have an ability to easily create covalent bonds with themselves and form larger systems, both ringed and linear. Although smaller acetylene chains are apt to self-reaction,[14] larger ones are predicted to be important intermediates toward the formation of soot and, thus, may display higher stability.[15,16]

It has been suggested that the degree of ionization in interstellar clouds could be quite large.[17] The ionization potentials of the polyacetylene hydrocarbon chains have been measured up to HC_8H, and the trend shows that diacetylene's value is 10.2 eV but that of all larger carbon chains is less than 9 eV.[18,19] Thus there may be a large abundance of such ionized species located in the diffuse clouds.

Electronic absorption spectra obtained in 6 K neon matrices already exist for the large acetylene cation series;[2] however, gas-phase values are needed for direct comparison with astrophysical observations. In this paper results utilizing a technique that has been recently developed in Basel for measuring the gas-phase spectrum of collisionally cooled ions using a 2-color 2-photon approach are presented.[20] Ions are typically cooled to vibrational and rotational temperatures on the order of 30−80 K, mimicking conditions that are relevant in diffuse interstellar clouds. Such low temperatures also eliminate the presence of vibrational hot bands, rendering assignments of the origin band straightforward.

Although the neutral polyacetylene chains have been well documented and studied up to $HC_{28}H$ in the gas phase,[14,21] the cations have only been studied up to $HC_{10}H^+$, with origin bands for HC_nH^+ ($n = 4, 6, 8$) having been rotationally resolved.[3−8] Those for $n = 10$ and greater will have rotational constants on the order of 0.01 cm^{-1} or less,[8] thus creating difficulties in trying to elucidate the spectroscopic structure of these larger chains.

Previous observations of the absorption spectra of the A $^2\Pi-X\ ^2\Pi$ transition for $HC_{12}H^+$, $HC_{14}H^+$, and $HC_{16}H^+$ in 6 K neon matrices locate the origin bands at 934.1, 1047.1, and 1159.8 nm, respectively.[2] Typically, the gas-phase transitions for smaller polyacetylene cations are blue-shifted by 100−130 cm^{-1} with respect to the neon matrix values.[8] Taking into account such shifts places these transitions at 923.1−925.7, 1033.3−1036.5, and 1142.9−1146.8 nm in the gas phase. As the number of carbon atoms increases, the strong A $^2\Pi-X\ ^2\Pi$ electronic transition of the polyacetylene cations shifts linearly (in nm) to the red.

Experimental Method

The apparatus has been described.[22] Ions are created using electron impact (12−30 eV, depending on the size of the carbon chain). A flow of diacetylene gas vapor is used as a precursor for the polyacetylene cations.

The newly created ions are mass selected by a quadrupole mass filter and are injected into a 3.6 cm long 22-pole ion trap, based on the design of Gerlich.[23] The quadrupole resolution was set to ±0.5 amu to prevent transmission of $C_{2n}H^+$ or $C_{2n}H_3^+$ species. The trap is loaded with approximately 30 000 ions in 20 ms (number of ions varied with the size of the carbon chain). In the trap ions undergo collisions with cryogenically cooled He buffer gas for 60 ms, thermalizing the trapped ions both rotationally and vibrationally.

Once sufficiently cooled, the ions are probed using a 2-photon 2-color pump−probe approach, with the excitation light being provided from both a tunable Nd:YAG pumped OPO laser (0.3 cm^{-1}) and the fixed double output from a broadband OPO system (6 cm^{-1}). Tunable radiation was used to promote an

* Corresponding author. E-mail: j.p.maier@unibas.ch. Phone: +41 61 267 38 26. Fax: +41 61 267 38 55.

10.1021/jp067439j CCC: $37.00
Published on Web 02/21/2007

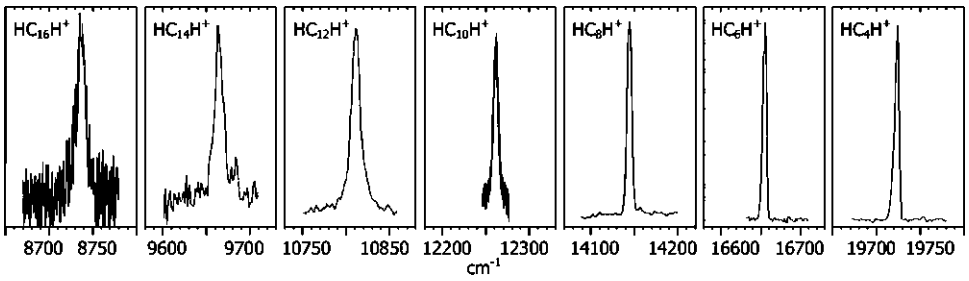

Figure 1. Gas-phase origin bands observed for the A $^2\Pi-X\ ^2\Pi$ transition of the $HC_{2n}H^+$ species.

TABLE 1: Observed Band Maxima (nm) for the A $^2\Pi-X\ ^2\Pi$ Polyacetylene Cation Series in the Gas Phase, the Estimated Oscillator Strengths f_{0-0}, and Inferred Upper Limits for the Column Densities N_{max} in Diffuse Clouds

species	transition	λ_{max}	f_{0-0}	$N_{max}/10^{12}$ cm^{-2}
HC_4H^+	A $^2\Pi_u-X\ ^2\Pi_g$	506.8	0.04[a]	1
HC_6H^+	A $^2\Pi_g-X\ ^2\Pi_u$	600.2	0.06[b]	0.5
HC_8H^+	A $^2\Pi_u-X\ ^2\Pi_g$	706.8	0.08[c]	0.3
$HC_{10}H^+$	A $^2\Pi_g-X\ ^2\Pi_u$	815.4	0.10[c]	0.2
$HC_{12}H^+$	A $^2\Pi_u-X\ ^2\Pi_g$	924.7	0.12[c]	0.1
$HC_{14}H^+$	A $^2\Pi_g-X\ ^2\Pi_u$	1034.6	0.14[c]	
$HC_{16}H^+$	A $^2\Pi_u-X\ ^2\Pi_g$	1144.0	0.16[c]	

[a] Reference 32. [b] Reference 19. [c] Estimated from trend (see text).

electronic excitation. A subsequent UV photon was then used to initiate fragmentation of the excited ions. For optimum signals the two laser beams must be overlapped in both time and space. Time overlap was monitored using two identical photodiodes; jitter was less then 10 ns. The experiment is run in pulsed mode at 10 Hz repetition.

After resonance excitation the newly dissociated products are released from the ion trap by lowering the exit potential. A second quadrupole filters the fragment ions, allowing only the product ions to be detected by a Daly detector. The spectra were obtained by monitoring the number of fragment ions as a function of photon energy. To obtain maximum signal, the resolution of the second quadrupole was decreased to allow all fragment ions (loss of C_3, C_3H, and C_3H_2) to be collected at once. The excitation laser alone produces no background. Running the UV fragmentation laser, however, does produce a background signal of a few counts. Signals are typically over an order of magnitude larger in intensity when at resonance using both lasers.

Results and Discussion

The origin bands observed for the A $^2\Pi-X\ ^2\Pi$ electronic transitions of HC_4H^+ through $HC_{16}H^+$ are shown in Figure 1 and are summarized in Table 1. The origin bands dominate the A $^2\Pi-X\ ^2\Pi$ system, and thus only these were searched for due to their astrophysical relevance. Other higher lying excited electronic states, as predicted by theory,[24] were not investigated here.

The observed bands are not rotationally resolved because the rotational constants vary from 0.15 cm^{-1} for HC_4H^+ to less than 0.01 cm^{-1} for species larger than $HC_{10}H^+$. The best laser resolution obtained was 0.3 cm^{-1}. In addition, lifetime broadening might occur as a result of intramolecular processes. A shift in the origin band to the red is observed as the number of carbon atoms in the chain increases (Figure 2). Simulating the rotational profile of HC_6H^+ using spectroscopic constants taken from the literature[8] and a line width of 0.3 cm^{-1} demonstrated that temperatures as low as 30 K were obtained (Figure 3).[25] Also of note is that photostability and oscillator strengths have been reported to increase with the number of carbon atoms as well.[8]

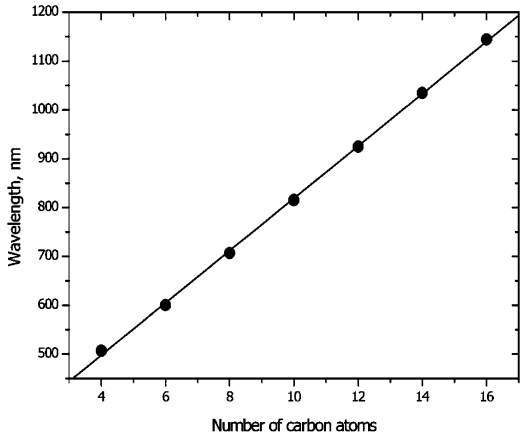

Figure 2. Linear relationship between the number of carbon atoms and the location of the origin band (A $^2\Pi-X\ ^2\Pi$) in the gas phase.

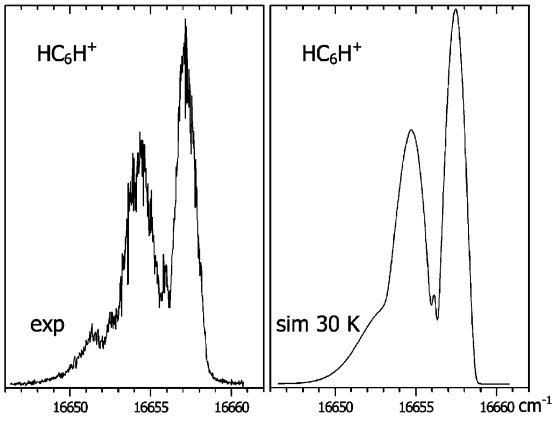

Figure 3. Simulation of the rotational profile for the A $^2\Pi_g-X\ ^2\Pi_u$ transition of HC_6H^+ demonstrating that temperatures of 30 K were obtained in the ion trap. Spectroscopic constants were taken from the literature,[8] and a line width of 0.3 cm^{-1} was used.

Two spin orbit origin bands, $^2\Pi_{3/2}-^2\Pi_{3/2}$ and $^2\Pi_{1/2}-^2\Pi_{1/2}$, are expected for a A $^2\Pi-X\ ^2\Pi$ transition. Their intensity ratio is determined by the temperature and the spin−orbit splitting in the ground state ($A'' \sim -33$ cm^{-1}).[24] The separation between the two bands is the difference in spin orbit constants in the excited and ground states ($\Delta A = A' - A'' \sim -3$ cm^{-1}), as observed for HC_4H^+ and HC_6H^+ in previous studies.[4] At 30 K the expected relative intensity of the $\Omega = {}^1/_2$ band will be 10−20% of $\Omega = {}^3/_2$ (20% Boltzmann determined and often the $\Omega = {}^1/_2$ components are less intense than the $\Omega = {}^3/_2$). Thus the $\Omega = {}^1/_2$ band is hidden under the unresolved P branch of the more intense A $^2\Pi_{3/2}-X\ ^2\Pi_{3/2}$ band in Figure 3 but is partially responsible for the substructure observed near 16 652 cm^{-1}, which lies ~3 cm^{-1} to the red of the $\Omega = {}^3/_2$ component.

Previous studies have shown that for HC_4H^+ approximately 80% of the ions in the $v' = 0$ level of the A $^2\Pi_u$ state fluoresce,

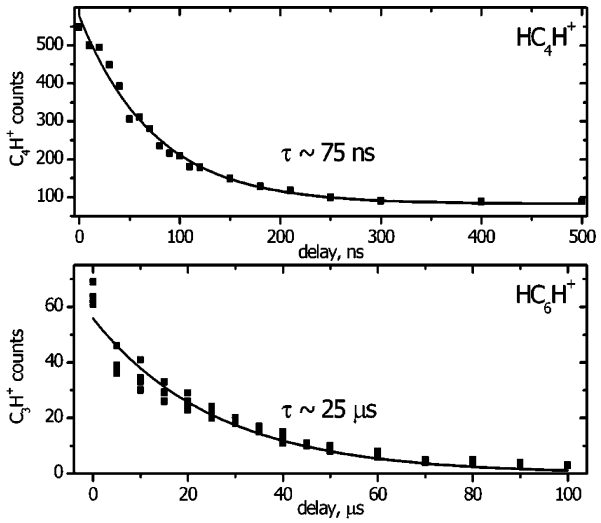

Figure 4. Cooling dynamics of HC_4H^+ and HC_6H^+ observed by varying the delay between pump (507 or 600 nm) and probe (210 or 248 nm) lasers while monitoring the intensity of the C_4H^+ or C_3H^+ fragment ions.

with minor channels losing energy through nonradiative processes.[19] The cited experiment measured fluorescent lifetimes of 71, 17, and <6 ns for the chain species HC_4H^+, HC_6H^+, and HC_8H^+, respectively. The quantum yield was also found to decrease as the chain size lengthened, indicating that the nonradiative channel of relaxation becomes more important as the size of the radical increases. These increasingly short lifetimes result in the broadened line widths observed as the chain length increases, as shown in Figure 1. This effect thus appears to outweigh any peak narrowing due to the decreased rotational profile contours of the longer chains.

The population of the excited species was probed by delaying the length of time between the excitation and fragmentation laser pulses. In the case of HC_4H^+ the A $^2\Pi$ state has a lifetime of 71 ns.[19] Thus the measured decay curve (upper trace of Figure 4) with a comparable time-constant shows that it is the A $^2\Pi$ excited-state which absorbs the UV photon leading to fragmentation. On the other hand, the A $^2\Pi$ excited-state lifetime is 17 ns for HC_6H^+, and even less for longer chains. However, the bottom curve in Figure 4 has a time constant $\sim$25 μs, thus demonstrating that an internal conversion from the A $^2\Pi$ excited state is the dominant process for chains HC_6H^+ and larger. The long decay curves observed in the trap may thus be attributed to a population of molecules either in the ground state's highly excited vibrational levels or in a close lying quartet state. For the polyacetylene cations the spin forbidden quartet states, $^4\Pi_u$ and $^4\Pi_g$, lie higher in energy in the linear geometry than the A $^2\Pi$ states that are accessed in this experiment, although calculations show that the quartet states drop closer toward the vicinity of the doublet states as the molecules bend.[24] Therefore the quartet states could play a role in the dynamics observed.

These results are similar to the findings observed when examining the B $^1A_1-X\ ^1A_1$ excited-state populations of the protonated polyacetylenes, $HC_nH_2^+$ of C_{2v} symmetry, in the same ion trap.[20] For the $HC_nH_2^+$, $n = 6$, 8, species it was concluded that an internal conversion process occurred on a subnanosecond time scale; whether the excited ions crossed into a lower lying triplet state or into the ground state's highly excited vibrational manifold could not be determined. TD−DFT calculations indicated that more than a few triplet states were accessible through an intersystem crossing from the B $^1A_1$ singlet state that was being probed.

In both cases the excited radicals lose their internal energy through collisions with the cooled helium buffer gas, resulting in a vibrational to translational energy transfer which gradually cools the ions. Given the background pressure of the buffer gas (approximately 4×10^{-4} mbar) and the size of the cold ion trap, an estimated 1 collision per microsecond occurs between the excited polyacetylene cation species and the helium gas.

Conclusions

The gas-phase A $^2\Pi-X\ ^2\Pi$ origin bands of seven different polyacetylene cation chains have been recorded, with $HC_{12}H^+$, $HC_{14}H^+$, and $HC_{16}H^+$ presented for the first time. A two-color two-photon pump−probe experiment was used to dissociate the polyatomic species in a 22-pole ion trap, which led to efficient cooling of the studied species through collisional relaxation with cryogenically cooled helium. This allows comparison of laboratory collected spectra to astrophysical observations. In this series the data for HC_4H^+ through HC_8H^+ were previously compared to the diffuse interstellar bands (DIB) literature and revealed no distinct matches.[26] A consultation of similar references[27−31] also yields no corresponding features for $HC_{10}H^+$. In the case of $HC_{12}H^+$, $HC_{14}H^+$, and $HC_{16}H^+$ the comparison is difficult due to the fact that there are few detectable DIBs reported longward of 800 nm. A recent study compiled DIB data up to 963 nm;[31] however no matches corresponding to the origin band of $HC_{12}H^+$ were found.

An upper limit to the column density for this series can be estimated from $N_{max}\ (cm^{-2}) = 1.13 \times 10^{20} W_{max}/\lambda^2 f$, where f is the oscillator strength of the electronic transition and W_{max} represents the equivalent width. Experimental oscillator strengths have been reported for HC_4H^+ and HC_6H^+ (Table 1).[19,32] Extrapolating this trend for longer chains yields $f_{0-0} = 0.08$, $f_{0-0} = 0.10$, and $f_{0-0} = 0.12$ for HC_8H^+, $HC_{10}H^+$, and $HC_{12}H^+$.[26,33] Using estimated equivalent widths $W_{max} = 10$ mÅ as the sensitivity limit for DIB detection in the visible region gives the upper limit column densities shown in Table 1.

Acknowledgment. This work has been supported by the Swiss National Science Foundation (grant 200020-100019) and is part of the European Union project "Molecular Universe" (MRTN-CT-2004-512303).

References and Notes

(1) Smith, A. M.; Agreiter, J.; Härtle, M.; Engel, C.; Bondybey, V. E. *Chem. Phys.* **1994**, *189*, 315.

(2) Freivogel, P.; Fulara, J.; Lessen, D.; Forney, D.; Maier, J. P. *Chem. Phys.* **1994**, *189*, 335.

(3) Lecoultre, J.; Maier, J. P.; Rosslein, M. *J. Chem. Phys.* **1988**, *89*, 6081.

(4) Klapstein, D.; Kuhn, R.; Maier, J. P.; Ochsner, M.; Zambach, W. *J. Phys. Chem.* **1984**, *88*, 5176.

(5) Sinclair, W. E.; Pfluger, D.; Linnartz, H.; Maier, J. P. *J. Chem. Phys.* **1999**, *110*, 296.

(6) Pfluger, D.; Sinclair, W. E.; Linnartz, H.; Maier, J. P. *Chem. Phys. Lett.* **1999**, *313*, 171.

(7) Pfluger, D.; Motylewski, T.; Linnartz, H.; Sinclair, W. E.; Maier, J. P. *Chem. Phys. Lett.* **2000**, *329*, 29.

(8) Cias, P.; Vaizert, O.; Denisov, A.; Mes, J.; Linnartz, H.; Maier, J. P. *J. Phys. Chem. A* **2002**, *106*, 9890.

(9) Homann, K. H. *Angew. Chem.-Int. Ed.* **1968**, *7*, 414.

(10) Tielens, A. G. G. M., Snow, T. P., Eds. Laboratory studies of proposed carriers. *The diffuse interstellar bands*; Kluwer Academic Publishers: Dordrecht, Netherlands, 1995; pp 175−238.

(11) McCarthy, M. C.; Travers, M. J.; Kovacs, A.; Gottlieb, C. A.; Thaddeus, P. *Astrophys. J. Suppl. Ser.* **1997**, *113*, 105.

(12) Shindo, F.; Benilan, Y.; Guillemin, J. C.; Chaquin, P.; Jolly, A.; Raulin, F. *Planet Space Sci.* **2003**, *51*, 9.

(13) Maier, J. P.; Walker, G. A. H.; Bohlender, D. A. *Astrophys. J.* **2004**, *602*, 286.

(14) Kloster-Jensen, E.; Haink, H.-J.; Christen, H. *Helv. Chim. Acta* **1974**, *57*, 1731.
(15) Stein, S. E.; Fahr, A. *J. Phys. Chem.* **1985**, *89*, 3714.
(16) Heath, J. R.; Zhang, Q.; O'Brien, S. C.; Curl, R. F.; Kroto, H. W.; Smalley, R. E. *J. Am. Chem. Soc.* **1987**, *109*, 359.
(17) Roberge, W. G.; Jones, D.; Lepp, S.; Dalgarno, A. *Astrophys. J. Suppl. Ser.* **1991**, *77*, 287.
(18) Allan, M.; Heilbronner, E.; Kloster-Jensen, E.; Maier, J. P. *Chem. Phys. Lett.* **1976**, *41*, 228.
(19) Allan, M.; Kloster-Jensen, E.; Maier, J. P. *Chem. Phys.* **1976**, *17*, 11.
(20) Dzhonson, A.; Jochnowitz, E. B.; Kim, E.; Maier, J. P. *J. Chem. Phys.* **2007**, *126*, 044301.
(21) Pino, P.; Ding, H.; Güthe, F; Maier, J. P. *J. Chem. Phys.* **2001**, *114*, 2208.
(22) Dzhonson, A.; Gerlich, D.; Bieske, E. J.; Maier, J. P. *J. Mol. Struct.* **2006**, *795*, 93.
(23) Gerlich, D. *Adv. Chem. Phys.* **1992**, *82*, 1.
(24) Komiha, N.; Rosmus, P.; Maier, J. P. *Mol. Phys.* **2006**, *104*, 3281.
(25) PGOPHER, a Program for Simulating Rotational Structure, C. M. Western, University of Bristol, http://pgopher.chm.bris.ac.uk.
(26) Motylewski, T.; Linnartz, H.; Vaizert, O.; Maier, J. P.; Galazutdinov, G. A.; Musaev, F. A.; Krelowski, J.; Walker, G. A. H.; Bohlender, D. A. *Astrophys. J.* **2000**, *531*, 312.
(27) Jenniskens, P.; Désert, F.-X. *Astron. Astrophys. Suppl. Ser.* **1994**, *106*, 39.
(28) Herbig, G. H. *Annu. Rev. Astron. Astrophys.* **1995**, *33*, 19.
(29) Tuairisg, S. O.; Cami, J.; Foing, B. H.; Sonnentrucker, P.; Ehrenfreund, P. *Astron. Astrophys. Suppl. Ser.* **2000**, *142*, 225.
(30) Galazutdinov, G. A.; Musaev, F. A.; Krelowski, J.; Walker, G. A. H. *Publ. Astron. Soc. Pac.* **2000**, *112*, 648.
(31) Cox, N. L. J.; Kaper, L.; Foing, B. H.; Ehrenfreund, P. *Astron. Astrophys.* **2005**, *438*, 187.
(32) Maier, J. P.; Thommen, F. *J. Chem. Phys.* **1980**, *73*, 5616.
(33) Watson, J. K. G. *Astrophys. J.* **1994**, *437*, 678.